

Lithographically Cut Single-Walled Carbon Nanotubes: Controlling Length Distribution and Introducing End-Group Functionality

Steven R. Lustig,* Edward D. Boyes, Roger H. French, Timothy D. Gierke, Mark A. Harmer, Paula B. Hietpas, Anand Jagota, R. Scott McLean, Greg P. Mitchell, G. Bibiana Onoa, and Kerry D. Sams

Central Research and Development, E.I. du Pont de Nemours & Co. Inc.,
Wilmington, Delaware 19880

Received April 11, 2003; Revised Manuscript Received June 9, 2003

ABSTRACT

Single-walled carbon nanotubes are efficiently cut to precise submicrometer lengths and very narrow length distributions. Chemical functional groups are placed selectively only at the ends without the nanotube walls being modified or damaged. The new methodology includes lithography to place protective photoresist patterns over the nanotubes and reactive ion etching to remove the unprotected nanostructure. This approach enables critical dimensional and chemical control for integrated nanodevice manufacturing based on chemical self-assembly under ambient conditions.

Although single-walled carbon nanotubes (SWNTs) exhibit many favorable electronic properties in isolated devices,^{1–7} there are still several basic and serious hurdles to overcome before they can be used in future high-performance, high-density electronics.⁸ The assembly of SWNTs in circuitry will clearly require accurate control on placing a SWNT with a specific band gap, length, and chemical structure as well as location. In principle, SWNTs could be grown where needed within an electronic device. Exciting patterning techniques have been reported for in situ catalyst placement with orientation-directed SWNT growth.^{9–14} However, this approach is still challenged for the fine control of catalyst seed placement, post-growth catalyst abatement, and control of the SWNT length and band gap. Alternatively, today SWNTs can be grown in bulk,¹ separated by electronic structure,^{15,16} and can then be placed selectively on a substrate.¹⁷ However, a critical remaining challenge in this approach is producing undamaged SWNTs cut to the precise lengths required for the device. Nanotubes are typically synthesized in bulk to polydisperse lengths on the order of micrometers. Here they are bound into macroscopic ropes and often intractably entangled. Cleaving these ropes is likely to facilitate greatly their purification, dispersion, chiral separation, and positioning within an electronic device. This letter describes a cutting methodology that can make the availability of precise length SWNTs both technically and

economically feasible. The ability to modify the ends with specific chemical functional groups while preserving the side walls is a unique capability of this approach.

We have developed a novel method to cut nanotubes that offers high yield and cut-length precision. The method does not require that the nanotubes be dispersed or oriented. The process protects the nanotubes from damage and modification except at the specific locations of cleavage. The method further permits selective end-group functionalization, ease of recovery, and facile scaling for industrial-scale implementation. We believe the method is sufficiently robust to be applicable for cutting nanotubes of different synthesis processes (e.g., HiPco, laser-oven, arc discharge, etc). The method is also applicable to many nanostructured materials for which one wishes to trim the shape or size and modify the peripheral chemical group functionality at the cutting surface. This robustness is attributed to the wide range of alternative lithography materials that can be used in the cutting process.

Previously reported methods to cut nanotubes provide very limited control over the precision of cutting and the protection of the remaining fragments. An early approach¹⁸ to cut nanotubes applied fast atom bombardment in high-vacuum chambers. Because all tubes are vulnerable to indiscriminate bombardment, much of the remaining residue is damaged. More recent approaches include degrading the nanotubes in concentrated, strong acids¹⁹ or acids with peroxide.²⁰ However, this approach also functionalizes the nanotube sidewalls

* Corresponding author. E-mail: Steve.R.Lustig@usa.dupont.com.
Phone: 302-695-3899.

along their length,²¹ which drastically changes their constitutive properties and produces a broad distribution of lengths. Sonication also induces shortening,^{22,23} but this process is quite damaging to the tube walls. Sonication in some mixtures produces several holes along the nanotube length, resulting in a “worm-eaten look”.^{24–26} Grinding and ball milling particularly in diamond^{27–29} or cyclodextrins³⁰ have been studied, but this approach also increases porosity^{27–29} and produces spurious functional groups.³¹ Shortened nanotubes may also be produced by degradation on reactive surfaces;³² however, the net yields are low. Scanning probe microscopy offers very precise cutting and nicking of nanotubes,^{33–36} but these methods require that each nanotube be individually separated and laboriously mapped in advance. This approach is not yet readily amenable to cutting significant quantities of nanotubes expediently. More recently, Smalley and co-workers³⁷ have shown that chemical fluorination followed by pyrolysis provides modified, cleaved fragments with broad length distributions. We believe currently that none of these approaches would be economically feasible for bulk quantity synthesis of controlled-length SWNTs in commodity electronic devices.

Our method employs microlithography technology³⁸ coupled with reactive ion etching. The cutting process for nanotubes is described herein and illustrated in Scheme 1. The method begins by mobilizing nanotubes in a fluid that enables

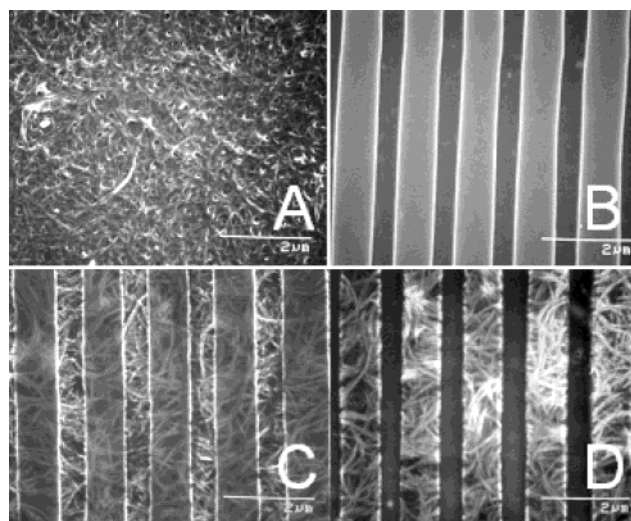
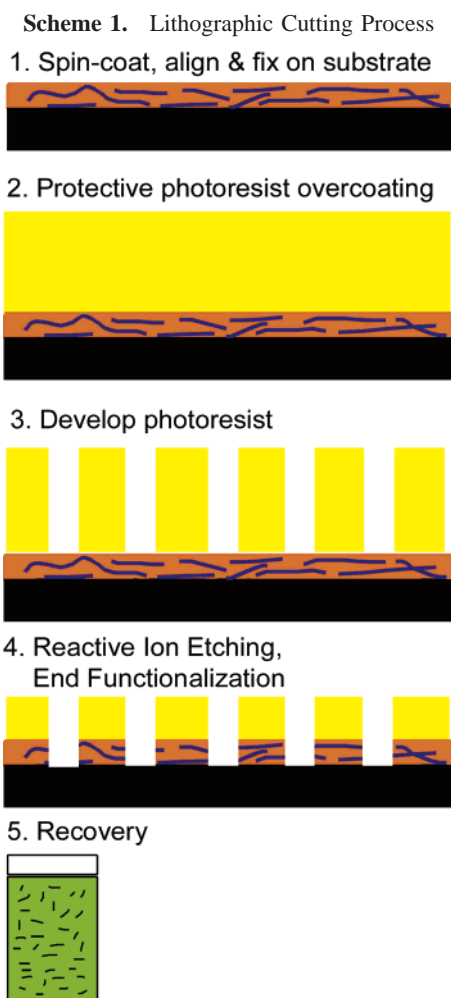


Figure 1. Scanning electron micrographs of (A) a random SWNT mat on a silicon wafer, (B) a control wafer with resist grating lines (no SWNTs), (C) a random SWNT mat underneath a resist grating with partially cut SWNTs after a 30-s plasma exposure, and (D) same as C after a 90-s exposure to yield the complete cutting of SWNTs embedded and protected in the resist

spreading on the surface of a suitable solid substrate, such as a standard silicon wafer or continuous belt. This layer is then covered with a photoresist polymer, usually by spin-coating or dip-coating. Light emanating from a photomask provides a spatial pattern (e.g., narrow parallel lines) of the photochemical reaction that defines which photoresist areas will be removed or preserved when the photoresist is developed. After the photoresist is developed, a portion of the nanotube population is exposed on the substrate according to the photomask pattern. An oxygen plasma now obliterates only the exposed nanotube portions. Note that portions of nanotubes underneath the resist pattern remain protected from etching and damage. At this point, only the nanotube ends remain exposed at the cutting planes and can be subjected to further chemical modification or functionalization. After exposure to an oxygen plasma, the SWNT ends will have carbon–oxygen chemical groups such as carboxylic acids and ethers. In the final step, we wash away the remaining resist pattern and resuspend the cut nanotubes.

The scanning electron micrographs in Figure 1 illustrate the key facets of the sample preparation and synthesis. All SWNTs used in this work were raw HiPco products obtained directly from Carbon Nanotechnologies Inc. This material was heated in air at 250 °C overnight, soaked in concentrated nitric acid at room temperature for 1 h with minimum, low-power sonication to wet the material and dissolve metal catalyst particles, filtered through sintered glass, washed with water, and dried under ambient conditions. The micrograph in Figure 1A is a typical random mat formed by spin-coating a 0.3 wt % dispersion of purified HiPco SWNTs in 1:1 chloroform/dichlorobenzene on a 4-in. silicon wafer at 1000 rpm. Figure 1B exhibits a control silicon wafer with a linear grating of photoresist. Shipley UVN30 DUV negative resist was spun on the wafer at 2800 rpm and baked for 60 s at 135 °C. The coated wafer was exposed through a standard resolution pattern photomask with 248-nm light at an

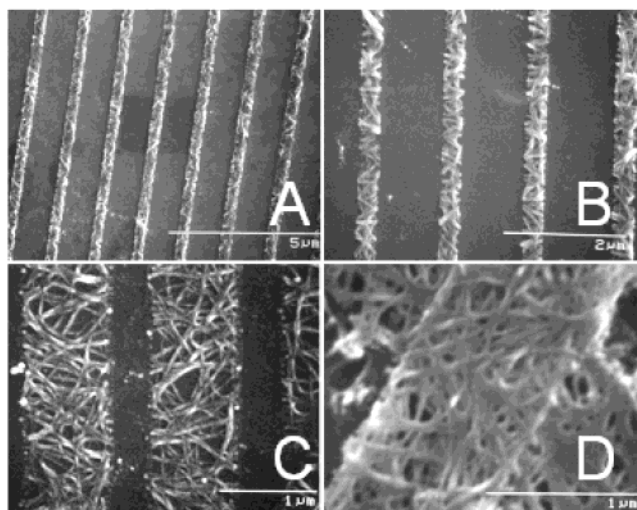


Figure 2. Scanning electron micrographs of a SWNT for (A) complete cutting from a negative resist grating in 30 s of plasma exposure with resist lift-off using NMP, (B) a higher magnification of A, (C) same as in Figure 1D where the resist has been stripped away using Nanostrip, and (D) recovered cut SWNTs from C via solvent (*N*-methylpyrrolidinone) washing of the resist and subsequent Nanostrip treatment for 1 h and collection on a Millipore 0.1- μm filter).

intensity of 55 mJ/cm^2 using a Nikon NSR-1505 EX-1 DUV 248-nm excimer laser stepper. The wafer was next baked at 130°C for 90 s and developed in AZ300 MIF for 60 s, rinsed in water, and dried. The resulting pattern of photoresist has 800-nm-wide protection lines and 400-nm-wide cutting lines. Here the narrower dark lines are the cutting channels exposing the substrate. The wider, elevated, light-gray lines are elevated strips of protective photoresist. Figure 1, micrographs C and D are sample wafers containing a bottom spin-coated SWNT mat and a top positive photoresist patterned identically to the Figure 1B control, although now the exposed nanotubes were cut by 90-W oxygen plasma at 30 mTorr in an Applied Materials reactive ion etcher. Micrograph 1C shows the effect of 60-s exposure to oxygen plasma. Note that several uncut SWNT fragments still remain exposed in the narrow channels and that the protected SWNT segments are visible through the resist by secondary electron emission within the SEM. The sample shown in Figure 1D shows that the SWNTs have been completely cut after 90-s exposure to oxygen plasma. Figure 2 shows SWNT cutting using a negative resist, illustrating a shorter cut dimension where the photoresist has been removed using conventional lift-off techniques. We also show that the cut tubes can be removed from the resist (e.g., using either a simple 1-methoxy-2-propanol, *N*-methyl pyrrolidinone (NMP) lift-off solvents, or Nanostrip, resuspension in DMAC, and filtration). A more detailed investigation of recovery using a variety of methods is currently underway.

Figure 3 summarizes an atomic force microscopy study of the cut nanotubes shown in Figure 2. Tapping-mode AFM was used to obtain height and phase imaging data simultaneously on a Nanoscope IIIa AFM, Dimension 3000 (Digital Instruments, Santa Barbara, CA). Microfabricated cantilevers or silicon probes (Nanoprobes, Digital Instruments) with 125-

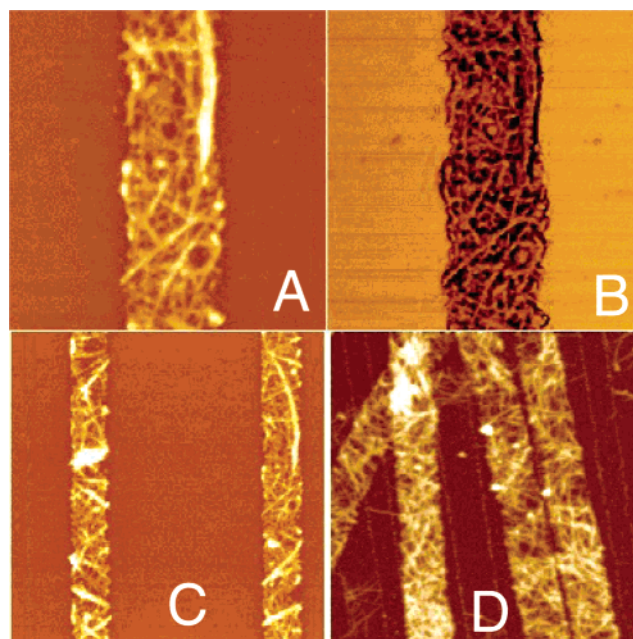


Figure 3. Tapping-mode AFM images of the sample shown in Figure 2C: (A) height mapping over a $1 \mu\text{m} \times 1 \mu\text{m}$ area. (B) phase data pertaining to A, (C) height mapping over an $8 \mu\text{m} \times 8 \mu\text{m}$ area, and (D) same as C after mild sonication.

μm -long cantilevers were used at their fundamental resonance frequencies, which typically varied from 270 to 350 kHz depending on the cantilever. Cantilevers had a very small tip radius of 5–10 nm. The AFM was operated under ambient conditions with a double vibration isolation system. Extender electronics were used to obtain height and phase information simultaneously. AFM data were obtained in tapping mode, in air, using previously described methods.³⁹ The images presented here are not filtered. AFM reveals that the resist is removed after processing, leaving behind intact cut bundles of CNTs. The bundles of CNTs were well protected by the resist lines during oxygen plasma etching. The edges of the cut CNT lines are well defined by the patterned resist lines. The height and phase images presented here are indistinguishable from CNT mats before being subjected to the cutting process. The data in this study supports the contention that the portions of nanotubes underneath the resist pattern remain protected from etching and damage. Thus, we expect that the middle sections of the CNTs are well preserved and would retain their spectroscopic and electronic properties.

If the nanotubes were perfectly oriented normal to the photoresist lines, then the nanotubes would be cut to lengths equal to the protective photoresist line width. Except for a minute population arising from the remaining original ends, the cut length distribution would be otherwise monodisperse. We note that there are several techniques that can be used to align nanotubes on surfaces.^{40–42} However, a general advantage of this process is that the nanotubes need not be particularly oriented or well-dispersed on the substrate to create a narrow and selective length distribution.

Even randomly oriented nanotubes are cut into very narrow length distributions using a linear grating photoresist. Figure

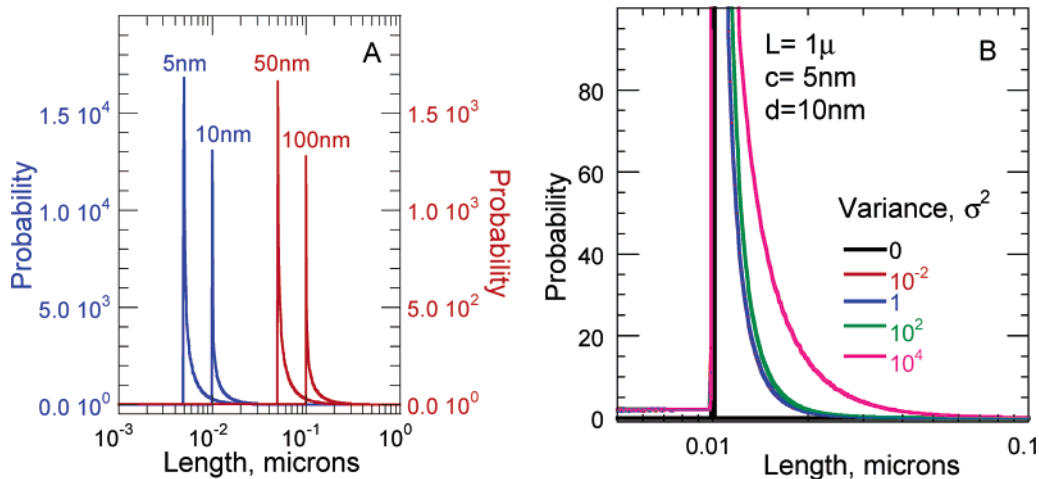


Figure 4. Predicted length probability distribution for SWNTs cut with linear grating photomask. (A) SWNTs with monodisperse 1- μm initial lengths with random orientation and 5-nm cutting lines. Distributions are shown for resist lines of 5, 10 (blue), 50, and 100 nm (red). (B) Distribution widths for various degrees of SWNT alignment variance normal to the linear grating.

4A illustrates cut length probability distributions predicted by geometric Monte Carlo computer simulation. The simulation samples random orientation angles between the photoresist lines and the SWNTs as well as the random offsets between the SWNT ends and the photoresist grating lines. For each statistical sample, the simulation itemizes how many sections are cut by a fixed grating and computes the resulting contributions to the length probability distribution. As long as the resist line width is much smaller than the original nanotube lengths, we note that the predicted length probability distribution is very sharply peaked at the photoresist width. Furthermore, the distribution width and shape are invariant on a logarithmic abscissa. Hence, the distribution is sensibly independent of the photoresist width. Simple geometric arguments provide an approximate analytic expression for the length probability distribution, $g(l)$, where probability distribution means number distribution, for randomly oriented SWNTs:

$$g(l) = \frac{2d}{\pi l} \left[\frac{L}{c + d} \frac{d}{l} \right] \frac{d}{\sqrt{l^2 - d^2}} \quad (1)$$

only for $l > d$, where d is the photoresist width, c is the width of the cutting line, and L is the original nanotube length. Within $0 \leq l < d$, the distribution is constant because of the original ends having a uniformly random placement under the linear protective photoresist grating. Note that the distribution is in fact singular at the length, l , equal to the photoresist width. In essence, those nanotubes originally oriented nearly normal to the resist lines contribute several fragments to the length distribution, but nanotubes originally oriented nearly parallel to the resist lines contribute far fewer fragments.

The length probability distribution resulting from a linear protective photoresist grating is remarkably insensitive to the starting-length distribution of the original, uncut SWNTs. Clearly, the cutting technique can be thought to broaden the length distribution if one starts with an SWNT ensemble with

monodisperse lengths. The distribution after cutting is still sharply peaked at the desired, shorter length. However, consider what happens if one starts with a very broad, uniform distribution of lengths, L , where $L_{\min} \leq L \leq L_{\max}$ and $c < d \ll L_{\min}$. Geometric Monte Carlo calculations show that the resulting distribution of cut lengths is visually indistinguishable from the distribution starting from a monodisperse ensemble with length equal to L_{\max} , especially for $l > d$. The longest SWNTs contribute significantly more cut sections than the shorter SWNTs, and the entire cut-length probability distribution is always normalized to have unit area. Hence, the cutting technique can be thought to contract the length distribution if one starts with an SWNT ensemble with a very broad distribution of lengths. In practice, we find that SWNTs in the bulk combine to form very long ropes where individual SWNTs randomly attach along the length of the rope. It is an advantage that this cutting technique produces a cut-length distribution that is rather insensitive to the lengths of both the initial individual SWNTs as well as their ropes.

Randomly oriented SWNTs cut from this process do indeed exhibit our expected narrow length distribution. In one example, randomly oriented SWNTs were cut using 285-nm photoresist line widths. The protective photoresist lines were removed, leaving a significant number of bare, cut nanotube fragments that had adhered to the silicon wafer substrate. Seven random SEM images of the substrate were recorded where cut fragments were visible. Tube-length probability distributions were recorded by the graphical image analysis of 370 tube bundles using their apparent relative bundle width as a statistical weight. All tube sections were noted to be straight. Linear sections are expected because the 285-nm photoresist width is much shorter than the Kuhn segment length of ca. 1.6 μm for single-walled carbon nanotubes.⁴³ The resulting length data were collected into 20 statistical bins, and the resulting probability distribution was normalized to unit area. Figure 5 compares these data to the simple theoretical result in eq 1 given the same number and width of statistical bins. Theory and experiment

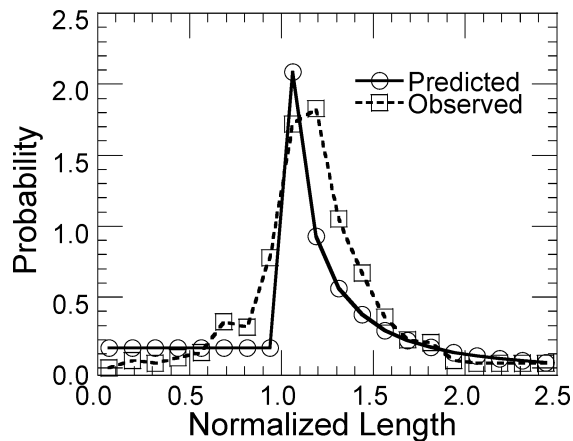


Figure 5. Comparison between the theoretical (eq 1) and observed length probability distributions; probability is a function of normalized length (l/d). The theoretical estimate was obtained assuming an initial length of $2.8 \mu\text{m}$.

are in very good agreement. In particular, the skewed nature of the length distribution and its width are captured well by the prediction. The discrepancy between the measured and predicted lengths is greatest at lengths just less than the photoresist width. In these preliminary efforts, the resist width varied roughly 5–10% along each resist line (Figure 1). We further note that the photoresist lines are reduced in width as well as in height during the oxygen plasma exposure. Better lithographic control of these line widths would produce an even narrower observed probability distribution.

The lithographic cutting technique clearly offers the ability to tailor the distribution by using different cutting patterns and by controlling the orientation of the nanotubes. For example, cutting with isolated photoresist circles results in a uniform distribution of lengths ranging from zero length to the diameter of the circle. Combined cutting by parallel lines and circles, on one photomask or with two sequential photomasks, will result in a distribution of lengths bounded by the line width and the circle diameter. A single photomask with a bimodal distribution of cutting patterns can be used to generate bimodal length distributions. Photomask patterns with splayed lines can generate controlled, broader length distributions. Furthermore, we estimate that even modest degrees of orientation can significantly sharpen the length distribution. Consider the following Gaussian orientation distribution function

$$P(\sigma^2, \theta) = \frac{8}{\pi(4 - \pi)} \sum_{n=1}^{\infty} \frac{(-1)^n}{2n + 1} \cos(2n\theta) \exp(-4n^2\sigma^2) + \frac{2}{\pi} \quad (2)$$

where θ is the orientation angle between the SWNT and the photoresist grating normal and σ^2 is the orientational variance. A variance as high as 100 deg^2 provides a broad distribution of orientations with a significant population of nanotubes that are nearly perpendicular to the photoresist grating. A variance as low as 10^4 deg^2 provides essentially a uniform distribution of orientations in the substrate plane. Figure 4B presents cut-length probability distributions pre-

dicted by geometric Monte Carlo simulation for different degrees of orientational variance. An orientational variance as high as 100 deg^2 still results in a distribution where ca. 90% of the cut tubes are within ca. 25% of the protection line width. An orientational variance of 10^4 deg^2 results in a distribution where ca. 70% of the cut tubes are with ca. 25% of the protection line width. Hence, even modest efforts to align the SWNTs would productively narrow the length distribution.

We envision two particular modifications to the methodology mentioned herein that would make this economically feasible for large-scale synthesis. First, replicated SWNT layers can multiply the yield capacity given essentially the same photoresist processing. It remains to be seen past how many SWNT layers the lithographic cutting will retain its fidelity. Second, interference lithography^{44–46} and spatial phase-locked electron beam lithography⁴⁷ seem quite promising. Such techniques can provide linear phase gratings that are high quality over a 10-cm^2 area. Furthermore these techniques are remarkably fast and low in cost. Given the availability of such technologies, we currently estimate that capacities of several dozen grams of synthesized SWNTs per day per process could be economically and technically feasible.

In summary, we have developed a unique cutting approach to developing SWNTs of controlled length. Although we have demonstrated this method using only HiPco SWNTs, we do anticipate that our cutting methodology will extend readily to other nanotubes, in particular, laser oven and CVD nanotubes, because there are many available alternatives for various steps in the process: dispersion, spinning onto the substrate, spinning on resist, and so forth. This method also offers the intriguing possibility of designing end-group reactivity while preserving the side walls and electronic properties. The rational design of single-walled carbon nanotubes with controlled length and structure will be a prerequisite to the use of these interesting materials for a wide variety of electronic applications.

Acknowledgment. This work was performed in part at the Cornell Nanofabrication Facility (a member of the National Nanofabrication Users Network), which is supported by the National Science Foundation under grant ECS-9731293, its users, Cornell University, and Industrial Affiliates.

References

- (1) Dresselhaus, M. S.; Dresselhaus, G.; Eklund, P. C. *Science of Fullerenes and Carbon Nanotubes*; Academic Press: San Diego, CA, 1996.
- (2) DePablo, P. J.; Graugnard, E.; Walsh, B.; Andres, R. P.; Datta, S.; Reifenberger, R. *Appl. Phys. Lett.* **1999**, *74*, 323–325.
- (3) Wei, Y. Y.; Eres, G. *Appl. Phys. Lett.* **2000**, *76*, 3759–3761.
- (4) Dai, H. J. *Surf. Sci.* **2002**, *500*, 218.
- (5) Wind, S. J.; Appenzeller, J.; Martel, R.; Derycke, V.; Avouris, Ph. *Appl. Phys. Lett.* **2002**, *80*, 3817.
- (6) Ouyang, M.; Huang, J. L.; Lieber, C. M. *Acc. Chem. Res.* **2002**, *35*, 1018.
- (7) Avouris, Ph. *Acc. Chem. Res.* **2002**, *35*, 1026.
- (8) *The International Technology Roadmap for Semiconductors 2002 Update* (available at <http://public.itrs.net>); European Semiconductor Industry Association, Japan Electronics and Information Technology Industries Association, Korea Semiconductor Industry Association, Taiwan Semiconductor Industry Association, Semiconductor Industry Association.

- (9) Li, W. Z.; Xie, S. S.; Qian, L. X.; Chang, B. H.; Zou, B. S.; Zhou, W. Y.; Zhao, R. A.; Wang, G. *Science* **1996**, *274*, 1701.
- (10) Li, J.; Papadopoulos, C.; Xu, J. M.; Moskovits, M. *Appl. Phys. Lett.* **1999**, *75*, 367.
- (11) Cassell, A. M.; Franklin, N. R.; Tomblor, T. W.; Chan, E. M.; Han, J.; Dai, H. J. *J. Am. Chem. Soc.* **1999**, *121*, 7975.
- (12) Joselevich, E.; Lieber, C. M. *Nano Lett.* **2002**, *2*, 1137.
- (13) Zhang, Y. G.; Chang, A. L.; Cao, J.; Wang, Q.; Kim, W.; Li, Y. M.; Morris, N.; Yenilmez, E.; Kong, J.; Dai, H. J. *Appl. Phys. Lett.* **2001**, *79*, 3155.
- (14) Huang, L.; Wind, S. J.; O'Brien, S. P. *Nano Lett.* **2003**, *3*, 299.
- (15) Chattopadhyay, D.; Galeska, I.; Papadimitrakopoulos, F. *J. Am. Chem. Soc.* **2003**, *125*, 3370.
- (16) Zheng, M.; Jagota, A.; Semke, E. D.; Diner, B. A.; Mclean, R. S.; Lustig, S. R.; Richardson, R. E.; Tassi, N. G. *Nature Mater.* **2003**, *2*, 338.
- (17) Wang, S.; Humphreys, E. S.; Chung, S. Y.; Delduco, D. F.; Lustig, S. R.; Wang, H.; Parker, K. N.; Rizzo, N. W.; Subramoney, S.; Chiang, Y. M.; Jagota, A. *Nature Mater.* **2003**, *2*, 196.
- (18) Anri, R. Kokai patent application HEI 7[1995]-172807.
- (19) Liu, J.; Rinzler, A. G.; Dai, H. J.; Hafner, J. H.; Bradley, R. K.; Boul, P. J.; Lu, A.; Iverson, T.; Shelimov, K.; Huffman, C. B.; Rodriguez-Macias, F.; Shon, Y.-S.; Lee, T. R.; Colbert, D. T.; Smalley, R. E. *Science* **1998**, *280*, 1253.
- (20) Stepanek, I.; De Menorval, L. C.; Edwards, R.; Bernier, P. *AIP Conf. Proc.* **1999**, *486*, 456.
- (21) Kuznetsova, A.; Popova, I.; Yates, J. T., Jr.; Bronikowski, M. J.; Huffman, C. B.; Liu, J.; Smalley, R. E.; Hwu, H. H.; Chen, J. G. *J. Am. Chem. Soc.* **2001**, *123*, 10699.
- (22) Shelimov, K. B.; Rinat, O.; Andrew, A. G.; Huffman, C. B.; Smalley, R. E. *Chem. Phys. Lett.* **1998**, *282*, 429.
- (23) Yanagi, H.; Sawada, E.; Manivannan, A.; Nagahara, L. A. *Appl. Phys. Lett.* **2001**, *78*, 1355.
- (24) Yudasaka, M.; Zhang, M.; Jabs, C.; Iijima, S. *Appl. Phys. A* **2000**, *71*, 449.
- (25) Zhang, M.; Yudasaka, M.; Koshio, A.; Jabs, C.; Ichihashi, T.; Iijima, S. *Appl. Phys. A* **2002**, *74*, 7.
- (26) Zhang, M.; Yudasaka, M.; Koshio, A.; Iijima, S. *Chem. Phys. Lett.* **2001**, *349*, 25.
- (27) Stepanek, I.; Maurin, G.; Bernier, P.; Gavillet, J.; Loiseau, A. *Mater. Res. Soc. Symp. Proc.* **2000**, *593*, 119.
- (28) Stepanek, I.; Maurin, G.; Bernier, P.; Gavillet, J.; Loiseau, A.; Edwards, R.; Jaschinski, O. *Chem. Phys. Lett.* **2000**, *331*, 125.
- (29) Maurin, G.; Stepanek, I.; Bernier, P.; Colomer, J. F.; Nagy, J. B.; Henn, F. *Carbon* **2001**, *39*, 1273.
- (30) Chen, J.; Dyer, M. J.; Yu, M. F. *J. Am. Chem. Soc.* **2001**, *123*, 6201.
- (31) Niesz, K.; Nagy, J. B.; Fonseca, A.; Willems, I.; Konya, Z.; Vesselenyi, I.; Mehn, D.; Bister, G.; Kiricsi, I. *AIP Conf. Proc.* **2001**, *591*, 345.
- (32) Zhang, Y.; Iijima, S. *Appl. Phys. Lett.* **2000**, *77*, 966.
- (33) Rubio, A.; Apell, S. P.; Venema, L. C.; Dekker, C. *Eur. Phys. J. B* **2000**, *17*, 301.
- (34) Kuzumaki, T.; Sawada, H.; Ichinose, H.; Horiike, Y.; Kizuka, T. *Appl. Phys. Lett.* **2001**, *79*, 4580.
- (35) Park, J.-Y.; Yaish, Y.; Brink, M.; Rosenblatt, S.; McEuen, P. L. *Appl. Phys. Lett.* **2002**, *80*, 4446.
- (36) Yoneya, N.; Watanabe, E.; Tsukagoshi, K.; Aoyagi, Y. *Appl. Phys. Lett.* **2001**, *79*, 1465.
- (37) Gu, Z.; Peng, H.; Hauge, R. H.; Smalley, R. E.; Margrave, J. L. *Nano Lett.* **2002**, *2*, 1009.
- (38) For example, see Moreau, W. M. *Semiconductor Lithography: Principles and Materials*; Plenum: New York, 1988.
- (39) McLean, R. S.; Sauer, B. B. *J. Polym. Sci., Part B: Polym. Phys.* **1999**, *37*, 859-866.
- (40) Gerdes, S.; Ondarcuhu, T.; Cholet, S.; Joachim, C. *Europhys. Lett.* **1999**, *48*, 292.
- (41) Vigolo, B.; Penicaud, A.; Coulon, C.; Sauder, C.; Pailler, R.; Journet, C.; Poulin, P. *Science* **2000**, *290*, 1331.
- (42) Yamamoto, K.; Akita, S.; Nakayama, Y. *Jpn. J. Appl. Phys., Part 2* **1996**, *35*, L917.
- (43) Sano, M.; Karnino, A.; Okamura, J.; Shinkai, S. *Science* **2001**, *293*, 1299.
- (44) Smith, H. I. *Physica E* **2001**, *11*, 104.
- (45) Schattenburg, M. L.; Chen, C.; Everett, P. N.; Ferrera, J.; Konkola, P.; Smith, H. I. *J. Vac. Sci. Technol., B* **1999**, *17*, 2692.
- (46) Savas, T. A.; Schattenburg, M. L.; Carter, J. M.; Smith, H. I. *J. Vac. Sci. Technol., B* **1996**, *14*, 4167.
- (47) Hastings, J. T.; Zhang, F.; Goodberlet, J.; Smith, H. I. *J. Vac. Sci. Technol., B* **2000**, *18*, 3268.

NL034219Y